

**Highly deformed Bands in  $^{175}\text{Hf}$** 

D. T. Scholes,<sup>1</sup> D. M. Cullen,<sup>1</sup> F. G. Kondev,<sup>2</sup> R. V. F. Janssens,<sup>3</sup> M. P. Carpenter,<sup>3</sup> D. J. Hartley,<sup>4,\*</sup> M. K. Djongolov,<sup>5</sup> G. Sletten,<sup>6</sup> G. Hagemann,<sup>6</sup> C. Wheldon,<sup>7</sup> P. M. Walker,<sup>7</sup> K. Abu Saleem,<sup>3</sup> I. Ahmad,<sup>3</sup> D. L. Balabanski,<sup>5</sup> P. Chowdhury,<sup>8</sup> M. Danchev,<sup>5</sup> G. D. Dracoulis,<sup>9</sup> H. M. El-Masri,<sup>7</sup> J. Goon,<sup>5</sup> A. Heinz,<sup>3</sup> R. A. Kaye,<sup>10</sup> T. L. Khoo,<sup>3</sup> T. Lauritsen,<sup>3</sup> C. J. Lister,<sup>3</sup> E. F. Moore,<sup>3</sup> L. L. Riedinger,<sup>5</sup> M. A. Riley,<sup>11</sup> D. Seweryniak,<sup>3</sup> I. Shestakova,<sup>8</sup> I. Wiedenhöver,<sup>3</sup> O. Zeidan,<sup>5</sup> and Jing-ye Zhang<sup>5</sup>

<sup>1</sup>*Schuster Laboratory, University of Manchester, Manchester M13 9PL, United Kingdom*

<sup>2</sup>*Nuclear Engineering, Argonne National Laboratory, Argonne, Illinois 60439, USA*

<sup>3</sup>*Physics Division, Argonne National Laboratory, Argonne, Illinois 60439, USA*

<sup>4</sup>*Department of Physics and Astronomy, University of Tennessee, Knoxville, Tennessee 37996, USA*

<sup>5</sup>*Department of Physics and Astronomy, University of Tennessee, Knoxville, Tennessee 37996, USA*

<sup>6</sup>*Niels Bohr Institute, Blegdamsvej 17, DK-2100, Copenhagen, Denmark*

<sup>7</sup>*Department of Physics, University of Surrey, Guildford GU2 7XH, United Kingdom*

<sup>8</sup>*Department of Physics, University of Massachusetts, Lowell, Massachusetts 01854, USA*

<sup>9</sup>*Department of Nuclear Physics, Australian National University, Canberra, Australian Capital Territory 0200, Australia*

<sup>10</sup>*Department of Chemistry and Physics, Purdue University, Calumet, Hammond, Indiana 46323, USA*

<sup>11</sup>*Department of Physics, Florida State University, Tallahassee, Florida 32306, USA*

(Received 4 August 2004; published 18 November 2004)

Two high-spin regularly spaced rotational bands with large dynamical moments of inertia have been identified in  $^{175}\text{Hf}$  with the Gammasphere spectrometer. These new bands are very similar to the previously identified triaxial superdeformed bands in the hafnium nuclei. However, the new bands in  $^{175}\text{Hf}$  have been linked into the known level scheme and thereby provide the first firm spin assignments for these structures in this region. In order to understand the new bands, theoretical calculations have been performed based on the ULTIMATE CRANKER code. The new bands in  $^{175}\text{Hf}$  are deduced to be built upon highly deformed structures. No experimental evidence for triaxiality was established and this work suggests that the structure of the so-called “triaxial” superdeformed bands in the Hf nuclei may be quite different from those identified in the lighter mass Lu nuclei. Since the two highly deformed bands in  $^{175}\text{Hf}$  are associated with different deformations, this work also identifies the role of the intruder orbits in polarizing the nuclear shape.

DOI: 10.1103/PhysRevC.70.054314

PACS number(s): 21.10.Re, 23.20.Lv, 27.70.+q

**I. INTRODUCTION**

To date, many regions of highly deformed or superdeformed nuclei have been established throughout the nuclear chart [1]. These collective rotational bands are based upon the occupation of so-called intruder orbit configurations. The intruder orbits have a large component of nuclear spin on the intrinsic body-fixed rotational axis of the nucleus and their excitation energy, relative to the Fermi level, decreases rapidly with increasing deformation and/or rotational frequency. As these intruder orbits descend toward the Fermi surface they help create shell gaps. The extra stability of these gaps is known to contribute to the stabilization of axially symmetric superdeformed nuclear shapes [2].

One of the successes of nuclear theory has been its ability to explain why a nucleus can assume a variety of shapes and even to predict where in the nuclear chart these different shapes would occur. Most of these shapes have predominantly been axially symmetric in nature, although this is not always the case. For example, recent evidence has been proposed that triaxial superdeformed (TSD) bands are based on

the development of single-particle triaxial shell gaps in non-axially-deformed nuclei [3]. The localization of these shell gaps through experimental evidence, therefore, provides important information about the deformation driving intruder orbitals.

In the past, establishing the presence of triaxial structures has proved experimentally difficult. In spite of this, nuclear triaxiality has been invoked to describe various phenomena, for example, anomalous signature splittings [4] and inversions [5] and chiral twin bands [6,7]. A triaxial nucleus has moments of inertia that differ about all three of the intrinsic body-fixed axes. Such triaxial shapes allow a phenomenon known as the wobbling mode to occur [8]. In this wobbling mode, the resulting rotational bands have the same basic rotational structure as regular collective rotational bands about the axis with the largest moment of inertia. However, wobbling bands have additional quanta of rotation about the other body-fixed axes. The main theoretical difficulties have been in predicting the exact locations of these shell gaps. In 1985 triaxial superdeformed bands were postulated in Ref. [9] and later discovered in  $^{163}_{71}\text{Lu}$  [10]. Direct evidence that these bands in  $^{163}_{71}\text{Lu}$  were indeed triaxial resulted from the observation of the wobbling mode [10]. In this case the properties of the electromagnetic transitions associated with the wobbling mode were in agreement with theoretical values based on the particle-rotor model [10].

\*Present address: Department of Physics, United States Naval Academy, Annapolis, MD 21402, USA.

In an attempt to understand the triaxial superdeformed bands in the Lu nuclei, Schnack-Petersen *et al.* [3] carried out a series of ULTIMATE CRANKER calculations [11–13]. These authors concluded that the  $N=94$  shell gap was responsible for stabilizing the triaxial structures in the mass 160 region. However, the calculations suggested that the triaxial shapes in  $^{163}\text{Lu}$  are not unique and that similar structures are likely to occur in other nuclei in the  $A \approx 165$  region. To date, TSD bands have been established in the (odd- $Z$ ) Lu isotopes  $^{161}\text{Lu}$ ,  $^{162}\text{Lu}$  [14],  $^{163}\text{Lu}$  [3,10,15–17],  $^{164}\text{Lu}$  [18],  $^{165}\text{Lu}$  [3,19,20], and  $^{167}\text{Lu}$  [21,22]. Attempts to find TSD bands in the even- $Z$  nuclei have, however, had mixed results. The predicted bands in  $^{164}\text{Hf}$  and  $^{166}\text{Hf}$  have not been discovered, but candidate TSD bands were found in the heavier mass nuclei  $^{168}\text{Hf}$  [23],  $^{170}\text{Hf}$  [24], and  $^{174}\text{Hf}$  [25]; however, no evidence for the wobbling mode has been established, thus far.

In this work we present the first evidence for highly deformed bands in an even- $Z$ , odd- $A$  hafnium nucleus,  $^{175}\text{Hf}_{103}$ . Transitions observed in the new bands have regular  $\gamma$  ray energy spacings of  $\approx 59$  keV and these bands are linked into the known lower-spin level scheme yielding firm spin and parity assignments up to spin  $123/2$ . One of these new bands is isospectral to the candidate triaxial superdeformed band 1 in  $^{174}\text{Hf}$  [25]. In order to understand these bands, a series of theoretical calculations have been performed based on the ULTIMATE CRANKER code. These calculations predict the existence of triaxial superdeformed shell gaps with  $\gamma \geq 15^\circ$  for  $N=100$  and  $106$  which survive to high spin [25]. However, because the new bands are firmly linked into the known  $^{175}\text{Hf}$  level scheme, the present data show discrepancies when compared with the theoretical results which may not have been evident without this additional information. These discrepancies, and the nonobservation of wobbling bands, suggest that the newly identified highly deformed bands in the Hf nuclei ( $^{170}\text{Hf}$  [24],  $^{168}\text{Hf}$  [23], and  $^{174}\text{Hf}$  [25]) may not be based on triaxial-deformed states like those of the Lu isotopes in the slightly lighter mass 160 region.

## II. EXPERIMENTAL DETAILS

High-spin states in  $^{175}\text{Hf}$  were populated with the  $^{130}\text{Te}(^{48}\text{Ca}, 3n)$  reaction at a beam energy of 194 MeV. A thin  $\approx 0.5\text{-mg/cm}^2$  target of enriched  $^{130}\text{Te}$  deposited on a  $\approx 0.2\text{-mg/cm}^2$  Au backing was used with the beam entering through the gold layer. The  $^{48}\text{Ca}$  beam was provided by the Atlas facility at the Argonne National Laboratory and the  $\gamma$  rays were detected with the 101 Compton suppressed Ge detectors of the Gammasphere array [26]. The primary aim of the experiment was the observation of rotational levels above high- $K$  isomers in  $^{175}\text{Hf}$  and therefore the trigger condition required the presence of three or more suppressed detectors in prompt coincidence. In approximately one day of beam time  $\approx 5.5 \times 10^8$  events of multiplicity  $\geq 3$  were recorded. The data were sorted into a four-dimensional (4D) energy cube and analyzed using the RADWARE package [27]. Gated 2D matrices were also created to obtain cleaner subsets of the data with coincidence gates placed on either high- or low- $K$  transitions.

## III. EXPERIMENTAL RESULTS

The low-spin structure of  $^{175}\text{Hf}$ , including several high- $K$  bands, is well established [28–31]. ( $K$  is the projection of the intrinsic nuclear spin onto the nuclear symmetry axis.) In their analysis with the Tessa3 array, Gjørup *et al.* [29] found evidence for two regular rotational bands which they were unable to assign to a specific Hf isotope. In the present work, the same reaction as Gjørup *et al.* [29] has been employed; however, the use of the Gammasphere spectrometer has resulted in a data set with much higher statistics. Analysis of this data set has allowed these rotational bands to be fully established and linked into the known level scheme of  $^{175}\text{Hf}$ . Figure 1 presents the  $^{175}\text{Hf}$  partial level scheme associated with these bands.

Figure 2(a) is a result of a sum of double-coincidence gates taken from the 4D cube, containing the five lowest clean transitions from band 1 (658, 717, 776, 895, and 953 keV) with either the 365- or 448-keV transitions from the  $7/2^+$  [633] band. The spectrum shows the two sequences of collective transitions, band 1 (filled circles) and band 2 (open circles), and the  $7/2^+$  [633] band (open triangles) up to spin  $41/2\hbar$  and the  $1/2^-$  [521] band (filled squares) up to spin  $43/2\hbar$ . Figure 2(b) is a sum of double gates from the 4D cube gated on the five lowest clean transitions from band 1 with the 221-keV  $\gamma$  ray which depopulates the  $K^\pi=23/2^-$  band (down triangles) (see Fig. 1). Transitions in this high- $K$  band are also fed by the decay of these new bands up to a maximum spin of  $41/2\hbar$ . The high-spin extension of the  $K^\pi=23/2^-$  band is the subject of a forthcoming article [28]. The inset to Fig. 2(b) provides a high-energy spectrum of the top of band 2, from a sum of triple gates from the 4D cube (one of 658-, 717-, 775-, 894-, and 952-keV  $\gamma$  rays with two  $\gamma$  rays from the 863-, 915-, 968-, 1025-, 1084- and 1144-keV transitions). Both Figs. 2(a) and 2(b) display a number of additional transitions which result from the decay of these bands. These  $\gamma$  rays have been identified in this work as linking transitions from band 1 to (i) the  $1/2^-$  [521] band, (ii) the  $7/2^+$  [633] band, and (iii) the  $K^\pi=23/2^-$  band, (see Fig. 1). Figures 3(a) and 3(b) present sums of triple-gated spectra which demonstrate the coincidence relations of the new  $\gamma$  rays connecting bands 1 and 2. These triple gates are formed from the (717-, 776-, 836-keV gates) with the (895-, 953-, 1008-keV gates) and either the 812-keV [Fig. 3(a)] or the 819-keV [Fig. 3(b)] transitions, respectively. The absence of the 1051-keV  $\gamma$  ray from Fig. 3(a) demonstrates that the 812- and 1051-keV  $\gamma$  rays are not in coincidence with each other and take mutually exclusive decay routes. Similarly, in Fig. 3(b), the 1058-keV  $\gamma$  ray is absent which demonstrates that it is not in mutual coincidence with the 819-keV transition. These relations and  $\gamma$ -ray intensities were used to construct the partial level scheme for  $^{175}\text{Hf}$  (see Fig. 1).

The multipolarity of the transitions was obtained, where possible, using the method of directional correlation of oriented states (DCO) [32]. DCO ratios ( $R_{DCO}$ ) were calculated from

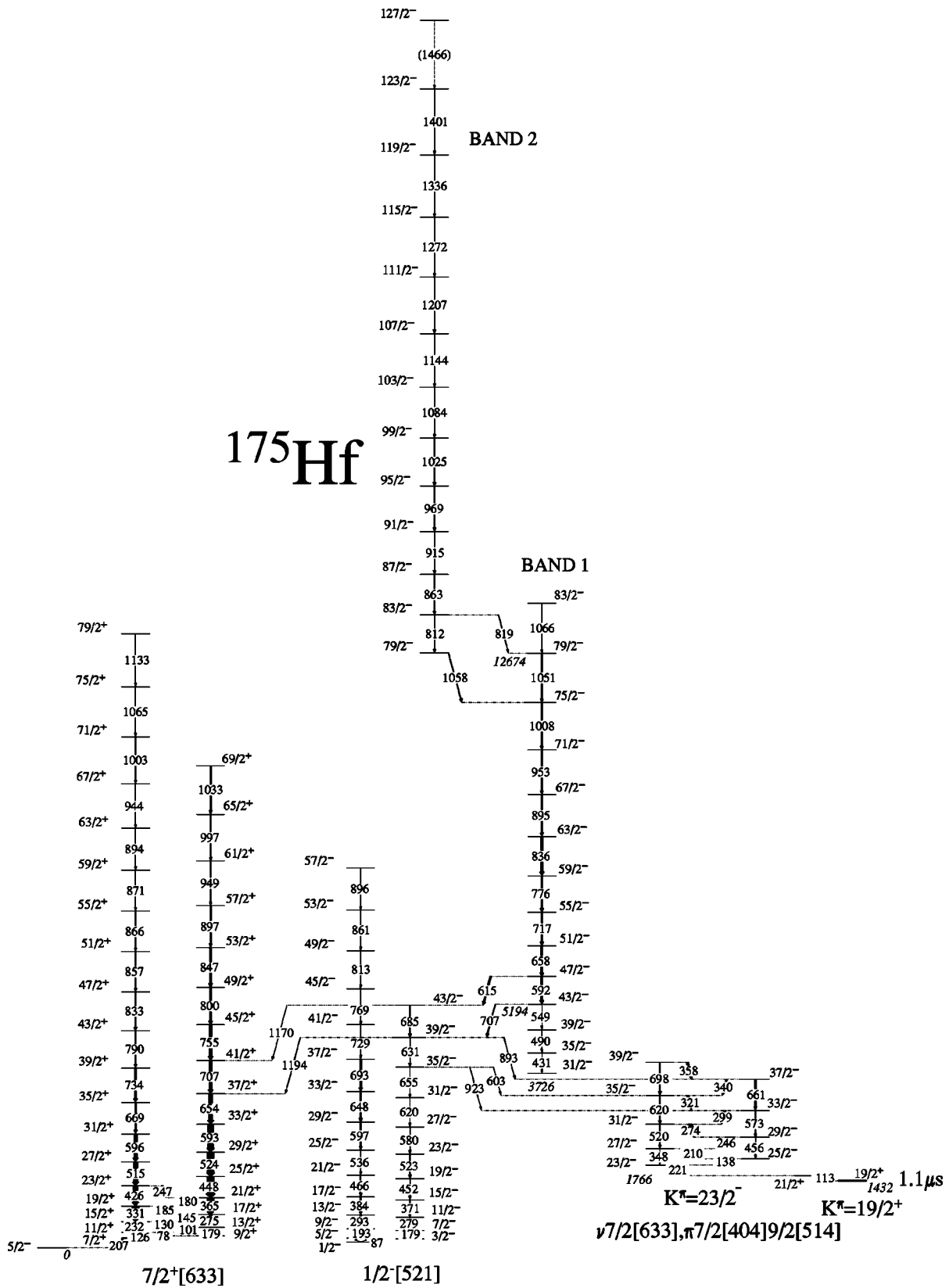


FIG. 1. Partial level scheme for  $^{175}\text{Hf}$ , showing the newly established collective bands and their decay through the  $1/2^- [521]$ ,  $7/2^+ [633]$ , and  $K^\pi=23/2^-$  bands.

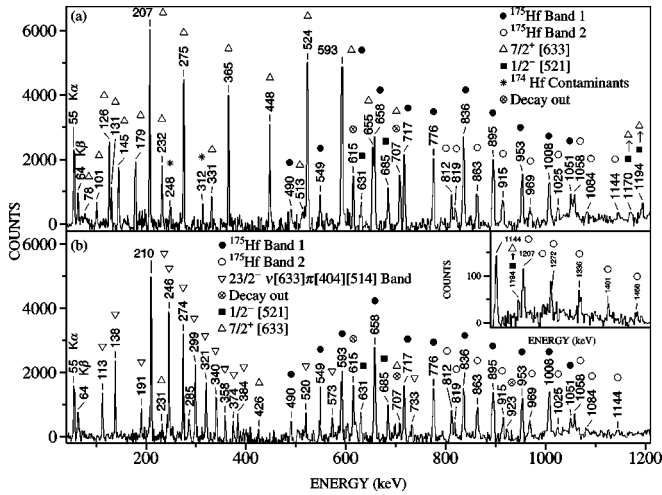


FIG. 2. Double-gated spectra from the 4D cube. (a) The five lowest clean transitions from band 1 with two transitions from the 7/2+ [633] band. Notice the population of the 1/2- [521] band (filled squares) and the transitions depopulating it (circles with crosses). (b) Gates on the 221-keV  $\gamma$  ray, from the  $K^\pi=23/2^-$  band and some transitions in band 1. This spectrum also shows the 1/2- [521] band (filled squares) and the feeding of the  $K^\pi=23/2^-$  band (down triangles) in  $^{175}\text{Hf}$ . Inset to Fig. 2(b) is a high-energy spectrum showing the top of band 2, from a sum of triple-gated spectra (see text for details).

$$R_{DCO} = \frac{I_\gamma(79^\circ, 81^\circ, 90^\circ, 100^\circ) \text{ gated by (all others)}}{I_\gamma(17^\circ, 32^\circ, 163^\circ, 148^\circ) \text{ gated by (all others)}}, \quad (1)$$

where  $I_\gamma$  is the number of counts in a fitted peak from a gated spectrum at the specified angles. These DCO ratios were then used to deduce the spins of the states. A DCO ratio of 1.0 in an  $E2$ -gated spectrum was interpreted as indicating that the

unknown transition was of stretched  $E2$  character, whereas a ratio of 0.5 was taken to correspond to a stretched  $\Delta I=1$  transition. These values were checked by measuring DCO ratios for some known transitions in the normal deformed 7/2+ [633] band in  $^{175}\text{Hf}$ . Table I gives the energies, intensities, DCO ratios, and assignments for bands 1 and 2 along with some established transitions [29].

For bands 1 and 2, the DCO ratios were measured from gates within the bands and assume that the 717-keV  $\gamma$  ray is an  $E2$  transition, which is likely given its position in the regular spacing of the energy levels. Under this assumption, the DCO analysis of the new  $\gamma$  rays shows that most are consistent with the behavior expected for  $E2$  transitions. In contrast, the 1170- and 1194-keV transitions, which are involved in the decay of band 1 to the 7/2+ [633] band through some intermediate states in the 1/2- [521] band, have DCO ratios which suggest they are dipole in nature and are consistent with stretched- $E1$  transitions. These transitions fix the spin and parity of the 3726-keV state in band 1 to be 31/2-. In agreement, two-state mixing is observed between the 1/2- [521] band and band 1 (see below), which is consistent with the DCO analysis in fixing the negative parity of band 1 to be the same as that of the 1/2- [521] band.

The spin and parity assignments for band 2 were deduced in a similar manner. The DCO ratios for the 812- and 819-keV transitions reveal that they are stretched- $E2$  transitions. This fixes the parity of band 2 to be negative and the 12 681-keV state to be 79/2-. This assignment is consistent with the fact that the 79/2- state in band 1 is established to be only 7 keV different in excitation energy from that of a 79/2- state in band 2 (see Fig. 1). These states mix (with a weak interaction strength of  $\approx 2.5$  keV) and this reveals that the spin and parity for bands 1 and 2 must be identical at the 79/2- level. In summary, this DCO analysis has allowed the spins and parties of the so-called TSD bands to be firmly established for the first time in the hafnium nuclei.

#### IV. DISCUSSION

The mid-shell-mass 170–180 nuclei are well known for their multi-quasiparticle excitations based on high- $K$  orbitals [33]. At low to moderate spins, these high- $K$  states are built upon prolate-deformed configurations with axial symmetry. At higher spins, recent calculations have shown that the intruder  $i_{13/2}$  proton orbit, and the  $j_{15/2}$  neutron orbit originating from above the  $N=126$  shell gap, may become occupied in, for example,  $^{174}\text{Hf}$  [25]. The occupation of such orbitals is expected to produce nuclear states with considerable deformation. At these high spins, the calculations also suggest that the hafnium nuclei become susceptible to triaxial deformation. Recently, evidence has been presented for several deformed rotational bands based on such nonaxial nuclear shapes in  $^{168}\text{Hf}$  [23],  $^{170}\text{Hf}$  [24], and  $^{174}\text{Hf}$  [25]. Unfortunately, unambiguous spins and parities could not be assigned to these bands because they were not linked into the known lower-spin level schemes. As such, comparisons with theoretical calculations to assign underlying single-particle configurations have been difficult.

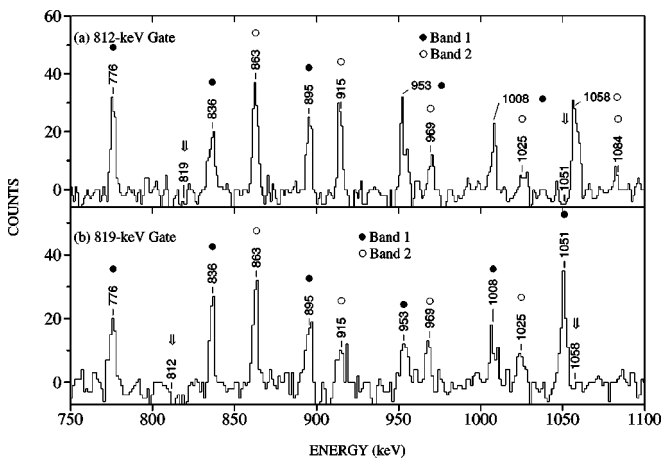


FIG. 3. Sums of triple-gated spectra containing the 717-, 776-, 836-keV  $\gamma$  rays with the 895-, 953-, 1008-keV  $\gamma$  rays and either the (a) 812-keV or (b) 819-keV transitions. The fact that the 1051-keV and the 1058-keV transitions are not in respective coincidence is clearly demonstrated, leading to the relative positioning of bands 1 and 2 shown in Fig. 1.

TABLE I. The energies, intensities, DCO ratios, and spin assignments for the  $\gamma$ -ray transitions in the new bands 1 and 2 and the normal deformed  $1/2^-$  [521] and  $7/2^+$  [633] bands in  $^{175}\text{Hf}$ . The DCO ratios were produced by gating on  $E2$  transitions; see text for details.

$E_\gamma$ (keV)	$I_\gamma$	$R_{DCO}$	Assignment	$I_i^\pi \rightarrow I_f^\pi$ ( $\hbar$ )
7/2 <sup>+</sup> [633] band				
101.2(1)	255(8)	0.45±0.19	$M1/E2$	13/2 <sup>+</sup> → 11/2 <sup>+</sup>
179.2(1)	281(8)	0.53±0.10	$M1/E2$	21/2 <sup>+</sup> → 19/2 <sup>+</sup>
186.2(1)	282(12)	0.37±0.14	$M1/E2$	19/2 <sup>+</sup> → 17/2 <sup>+</sup>
247.1(1)	224(11)	0.38±0.16	$M1/E2$	23/2 <sup>+</sup> → 21/2 <sup>+</sup>
365.4(1)	998(29)	0.90±0.11	$E2$	21/2 <sup>+</sup> → 17/2 <sup>+</sup>
447.9(1)	978(29)	1.22±0.01	$E2$	25/2 <sup>+</sup> → 21/2 <sup>+</sup>
523.7(1)	1000(30)	1.09±0.09	$E2$	29/2 <sup>+</sup> → 25/2 <sup>+</sup>
592.5(1)	719(23)	1.30±0.14	$E2$	33/2 <sup>+</sup> → 29/2 <sup>+</sup>
654.0(1)	561(17)	1.05±0.20	$E2$	37/2 <sup>+</sup> → 33/2 <sup>+</sup>
707.4(2)	448(18)	1.31±0.17	$E2$	41/2 <sup>+</sup> → 37/2 <sup>+</sup>
Band 1				
431(7)	8(4)		( $E2$ )	35/2 <sup>-</sup> → 31/2 <sup>-</sup>
489.5(5)	17(3)	1.21±0.21	$E2$	39/2 <sup>-</sup> → 35/2 <sup>-</sup>
548.9(4)	20(3)	1.11±0.11	$E2$	43/2 <sup>-</sup> → 39/2 <sup>-</sup>
591.8(4)	40(4)	1.09±0.05	$E2$	47/2 <sup>-</sup> → 43/2 <sup>-</sup>
658.1(5)	64(6)	0.94±0.07	$E2$	51/2 <sup>-</sup> → 47/2 <sup>-</sup>
716.9(8)	98(6)	1.06±0.07	$E2$	55/2 <sup>-</sup> → 51/2 <sup>-</sup>
775.8(4)	78(4)	1.01±0.06	$E2$	59/2 <sup>-</sup> → 55/2 <sup>-</sup>
836.1(9)	82(4)	0.94±0.06	$E2$	63/2 <sup>-</sup> → 59/2 <sup>-</sup>
895.3(5)	84(4)	1.18±0.05	$E2$	67/2 <sup>-</sup> → 63/2 <sup>-</sup>
953.3(6)	76(3)	1.18±0.06	$E2$	71/2 <sup>-</sup> → 67/2 <sup>-</sup>
1007.9(4)	92(4)	1.15±0.06	$E2$	75/2 <sup>-</sup> → 71/2 <sup>-</sup>
1050.8(9)	37(3)	1.10±0.08	$E2$	79/2 <sup>-</sup> → 75/2 <sup>-</sup>
818.8(9)	21(4)	1.00±0.21	$E2$	83/2 <sup>-</sup> → 79/2 <sup>-</sup>
1057.9(6)	51(4)	1.10±0.08	$E2$	79/2 <sup>-</sup> → 75/2 <sup>-</sup>
Band 2				
812.1(7)	19(3)	1.23±0.19	$E2$	83/2 <sup>-</sup> → 79/2 <sup>-</sup>
863.3(9)	33(3)	1.19±0.08	$E2$	87/2 <sup>-</sup> → 83/2 <sup>-</sup>
914.6(6)	34(3)	1.21±0.07	$E2$	91/2 <sup>-</sup> → 87/2 <sup>-</sup>
968.5(9)	19(3)	1.07±0.11	$E2$	95/2 <sup>-</sup> → 91/2 <sup>-</sup>
1024.7(7)	21(3)	1.19±0.13	$E2$	99/2 <sup>-</sup> → 95/2 <sup>-</sup>
1083.7(9)	17(3)	1.11±0.14	$E2$	103/2 <sup>-</sup> → 99/2 <sup>-</sup>
1144(1)	9(3)	1.04±0.21	$E2$	107/2 <sup>-</sup> → 103/2 <sup>-</sup>
1207(1)	8(3)		( $E2$ )	111/2 <sup>-</sup> → 107/2 <sup>-</sup>
1272(1)	4(2)		( $E2$ )	115/2 <sup>-</sup> → 111/2 <sup>-</sup>
1336(1)	4(2)		( $E2$ )	119/2 <sup>-</sup> → 115/2 <sup>-</sup>
1401(1)	4(3)		( $E2$ )	123/2 <sup>-</sup> → 119/2 <sup>-</sup>
1/2 <sup>-</sup> [521] Band				
614.8(7)	133(4)	0.96±0.08	$E2$	47/2 <sup>-</sup> → 43/2 <sup>-</sup>
630.8(7)	124(4)	1.16±0.11	$E2$	39/2 <sup>-</sup> → 35/2 <sup>-</sup>
684.7(7)	196(6)	1.17±0.12	$E2$	43/2 <sup>-</sup> → 39/2 <sup>-</sup>
707.3(7)	99(3)		( $E2$ )	43/2 <sup>-</sup> → 39/2 <sup>-</sup>
1169.9(7)	71(2)	0.42±0.15	$E1$	43/2 <sup>-</sup> → 41/2 <sup>+</sup>
1193.6(7)	196(3)	0.61±0.13	$E1$	39/2 <sup>-</sup> → 37/2 <sup>+</sup>

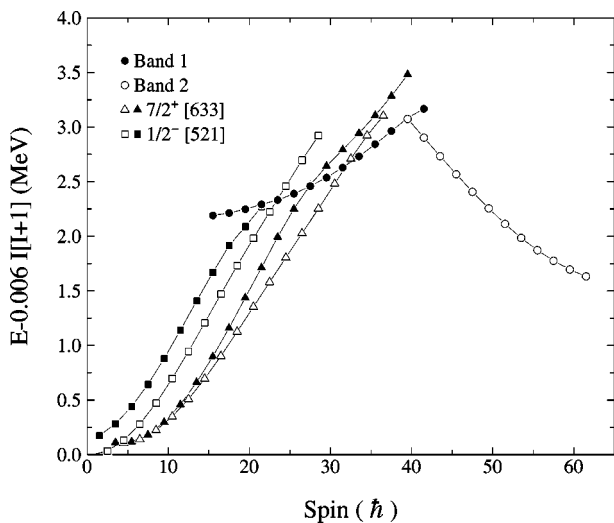


FIG. 4. Energy minus a rigid-rotor reference for the new bands 1 and 2 and some of the normal deformed bands in  $^{175}\text{Hf}$ .

In order to understand the population and decay of the new bands in  $^{175}\text{Hf}$ , their excitation energy (minus a reference) is plotted versus spin in Fig. 4. This reference term removes the collective contribution to the excitation energy.

Figure 4 indicates that the new band 2 (open circles) in  $^{175}\text{Hf}$  is yrast at high spin and thereby dominates the population intensity at this point. Band 2 has a large slope because of its large aligned angular momentum (see below). No other bands compete for this decay intensity until spin  $\approx 79/2\hbar$  where band 2 (open circles) is crossed by band 1 (closed circles) which becomes more yrast (see Fig. 4). Until this point, the large in-band  $B(E2)$  decay strength in band 2 dominates the competition for electromagnetic decays. However, the chance degeneracy of the  $79/2^-$  state in band 2 with that of band 1 provides an alternative decay path, at which point, the population intensity passes over to band 1. The large in-band  $B(E2)$  strength of the transitions in band 1 then carries the decay intensity until another chance degeneracy occurs with band 1 and the extension to the  $1/2^-$  [521] band (squares) at spin  $43/2\hbar$  in Fig. 4. Notice how the open squares of this band fall below those of band 1 (filled circles) below spin  $43/2$ . The new  $43/2\hbar$  state at 5195 keV is perturbed in energy due to mixing with the  $43/2\hbar$  state in band 1 at 5171 keV. The strength of this mixing was estimated to be  $\approx 10$  keV from the sizable perturbation in  $J^{(2)}$  value for band 1 at  $\hbar\omega \approx 0.25$  MeV in Fig. 7(b). This perturbation is also evident in the alignment plot for band 1 at  $\hbar\omega \approx 0.3$  MeV in Fig. 5.

The aligned angular momentum  $i_x$  (or alignment) for the new band 1 (filled circles,  $K=0.5$ ) and band 2 (open circles,  $K=0.5$ ) in  $^{175}\text{Hf}$  is presented in Fig. 5. In the figure, the alignment of these new bands is compared with that of the normal deformed  $5/2^-$  [512] (diamonds) and  $1/2^-$  [521] (squares) bands in  $^{175}\text{Hf}$  [28–31]. The other TSD bands in the hafnium nuclei are not shown because the spins of these bands are not established.

The two bands based on the one-quasiparticle  $5/2^-$  [512] and  $1/2^-$  [521] configurations in  $^{175}\text{Hf}$  are both affected by the first  $i_{13/2}$  band crossing at a rotational frequency of

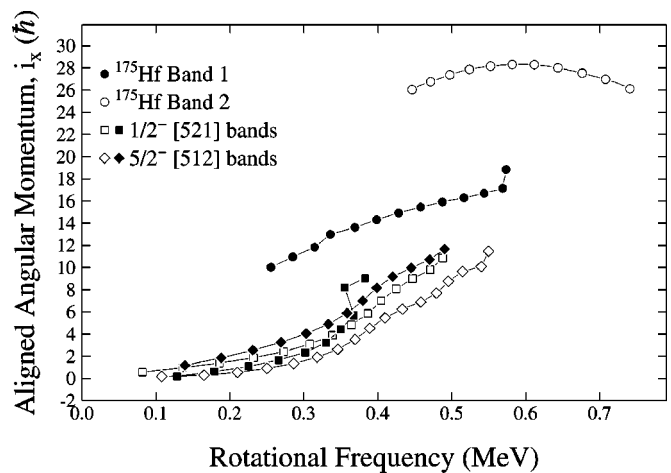


FIG. 5. The aligned angular momentum  $i_x$  for bands 1, 2, and the  $5/2^-$  [512] and  $1/2^-$  [521] bands in  $^{175}\text{Hf}$  [28–31]. Harris parameters  $J^{(0)}=30 \hbar^2/\text{MeV}$ ,  $J^{(1)}=40 \hbar^2/\text{MeV}^3$  were used.

$\approx 0.35$  MeV. This crossing introduces an alignment gain of approximately  $7\hbar$  in these bands, above which they are associated with three-quasiparticle configurations. In the  $1/2^-$  [521] bands, the  $+1/2$  signature (filled squares) shows a sharper crossing than the  $-1/2$  signature (open squares). This high-spin extension of the  $+1/2$  band structure was only identified from the decay of the new band 1 in this work and may be associated with a different intrinsic configuration in the region of the  $i_{13/2}$  neutron band crossing. Above this  $i_{13/2}$  crossing, the  $5/2^-$  [512] bands continue and are crossed once more by a five-quasiparticle configuration at a higher rotational frequency of  $\approx 0.5$  MeV. In comparison, the initial low-spin apparent alignment of band 1 ( $i_x \approx 10\hbar$ ) in  $^{175}\text{Hf}$  is larger than that of the  $1/2^-$  [521] and  $5/2^-$  [512] one-quasiparticle bands in  $^{175}\text{Hf}$  ( $i_x \approx 0\hbar$ ). This initial alignment of band 1 in  $^{175}\text{Hf}$  is sufficiently large that it may result from a five-quasiparticle configuration. Based on the available orbits around the Fermi surface, for a larger deformation ( $\epsilon_2 > 0.3$ ) than that of the normal-deformed bands, the most likely low-spin configuration for band 1 in  $^{175}\text{Hf}$  is  $\nu(h_{9/2})(i_{13/2})^2\pi(i_{13/2})^2$ . At a higher rotational frequency around 0.5 MeV, band 1 shows the start of a sharp upbend ( $\Delta i_x \approx 10\hbar$ ) where it is crossed by band 2. Such a large alignment gain is likely the result of a crossing involving a high- $j$  orbit such as a  $j_{15/2}$  neutron. In this case, band 2 would be based on a higher-order seven-quasiparticle structure. The most likely orbitals around the Fermi surface suggest that band 2 is based upon the  $\nu(h_{9/2})(i_{13/2})^2(j_{15/2})^2\pi(i_{13/2})^2$  configuration. Since band 2 in  $^{175}\text{Hf}$  is isospectral to the candidate triaxial superdeformed band 1 in  $^{174}\text{Hf}$  [25], then a similar configuration (less the additional  $h_{9/2}$  neutron) may well be responsible for this band in  $^{174}\text{Hf}$ . This likely revises the spin assignments and interpretations made for the TSD bands in  $^{174}\text{Hf}$  [25,34].

In order to assess the possible triaxial nature of the new bands in  $^{175}\text{Hf}$ , a series of potential energy surface (PES) calculations have been performed using the ULTIMATE CRANKER code [11–13,16]. Figure 6 shows the results of a PES calculation at  $I=99/2 \hbar$ , with parity and signature

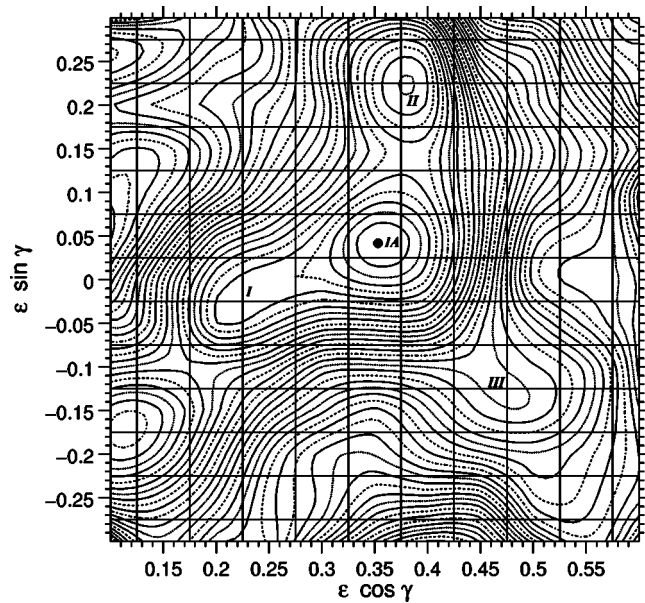


FIG. 6. Potential energy surface plot from the ULTIMATE CRANKER calculations for  $^{175}\text{Hf}$  based on the negative parity,  $\alpha = -1/2$  configuration at  $I = 99/2 \hbar$ . The contour interval is 200 keV.

$(\pi, \alpha) = (-, -1/2)$ . The calculation predicts several minima in the potential energy surface, all of which have large deformations as a consequence of the intruder orbital occupation. Using the labeling convention in Ref. [25], minimum IA in Fig. 6 occurs at  $(\varepsilon_2, \gamma) \approx (0.35, 5^\circ)$  and is the deepest at low spin. Minimum II lies  $\approx 200$  keV above minimum I at a larger deformation and with considerable triaxiality,  $(\varepsilon_2, \gamma) \approx (0.43, 35^\circ)$ . The third, more shallow minimum III occurs at  $(\varepsilon_2, \gamma) \approx (0.50, -15^\circ)$  with some triaxiality and a larger deformation. In this example calculation, any possible triaxial superdeformed band would be expected to be built upon minimum II in the potential energy surface in  $^{175}\text{Hf}$ . At high spin these calculations indicate that the lowest-energy structure in this minimum has a configuration based upon the  $\pi[(i_{13/2})^2, (h_{9/2})^2], \nu[(j_{15/2}), (i_{13/2})^2]$  orbitals. It should be noted though that in this high-spin region the alignment of a pair of low- $\Omega$ , high- $j$  quasiparticles may be overestimated due to insufficient quenching of pairing in the calculations. Unfortunately, the ULTIMATE CRANKER calculations, which were successfully employed in the lighter mass 160 region, do not provide unique solutions for the configurations of the new bands in  $^{175}\text{Hf}$ , since they do not predict the correct experimental deformation.

The deformation and configurations of these bands have been interpreted by considering the behavior of the dynamic moments of inertia [25]. Although the spin assignments for the other candidate TSD bands in  $^{168}\text{Hf}$  [23],  $^{170}\text{Hf}$  [24], and  $^{174}\text{Hf}$  [23] may need revising, the dynamic moments of inertia are not affected by these changes. Figure 7 demonstrates that the dynamic moments of inertia  $J^{(2)}$  for bands 1 and 2 in  $^{175}\text{Hf}$  observed in this work are large and are similar to those of the so-called TSD bands in  $^{168}\text{Hf}$  [23],  $^{170}\text{Hf}$  [24], and  $^{174}\text{Hf}$  [25].

All of the bands shown in Fig. 7(a) display a decreasing value of  $J^{(2)}$  with increasing rotational frequency. This is in

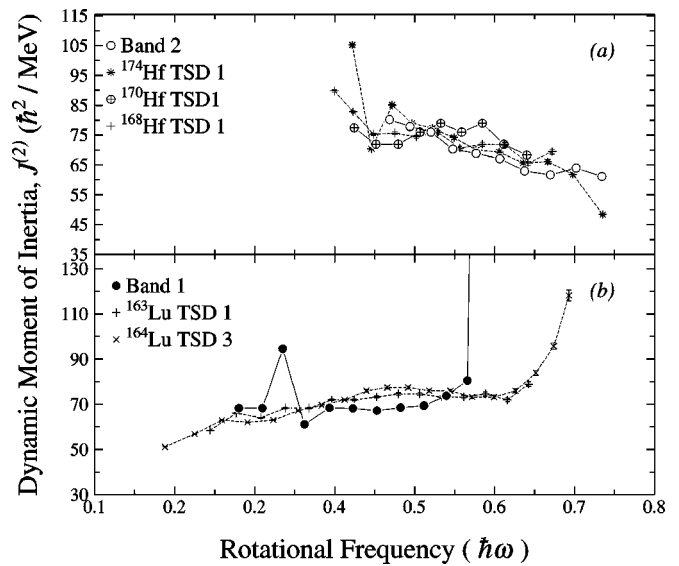


FIG. 7. Dynamic moments of inertia  $J^{(2)}$  for (a) band 2 in  $^{175}\text{Hf}$  and proposed TSD bands in  $^{168}\text{Hf}$  [23],  $^{170}\text{Hf}$  [24], and  $^{174}\text{Hf}$  [25], (b) band 1 and the  $7/2^+$  [633] band in  $^{175}\text{Hf}$  compared with known TSD bands in  $^{163}\text{Lu}$  [6] and  $^{164}\text{Lu}$  [18].

contrast to the behavior of band 1 and that of the TSD bands in the Lu isotopes,  $^{163}\text{Lu}$  [3] and  $^{164}\text{Lu}$  [18] shown in Fig. 7(b). These bands show an increase in  $J^{(2)}$  with increasing frequency. These observations show that there appear to be two classes of superdeformed bands in  $^{175}\text{Hf}$  based on their deformation. The new band 1 in  $^{175}\text{Hf}$  is similar to the triaxial superdeformed bands in the Lu nuclei, whereas band 2, and the other so-called TSD bands in  $^{168}\text{Hf}$  [23],  $^{170}\text{Hf}$  [24], and  $^{174}\text{Hf}$  [23], behave differently and are based on a larger deformation.

In order to test these ideas, experimental deformations have been extracted from the lifetimes of the states in bands 1 and 2. This method was used to confirm the deformed nature of the bands in  $^{174}\text{Hf}$  and  $^{168}\text{Hf}$  with values of  $Q_i \approx 13.5 e b$  [34] and  $Q_i = 11.4_{-1.2}^{+1.1} e b$  [23], respectively. Preliminary measurements for the quadrupole moments for the new bands in  $^{175}\text{Hf}$  [34] suggest that band 1 has  $Q_i \approx 9 e b$  and band 2 has  $Q_i \approx 13 e b$ . These experimental deformation measurements are consistent with the suggestion that band 2 is involved in a band crossing with band 1 where the additional two intruder orbitals lead to the larger deformation of band 2. However, the values predicted from the ULTIMATE CRANKER calculations are much smaller than those experimentally extracted for band 2 [34]. This discrepancy, in addition to the fact that multiple wobbling bands (one signature of triaxiality [8]) were not observed in this work, casts doubt on the interpretation that these bands in the hafnium nuclei are built upon triaxial shapes.

In the absence of a detailed explanation for the high deformation of band 2 in  $^{175}\text{Hf}$ , and by implication also in other hafnium isotopes, it is appropriate to draw attention to the prediction of “giant backbending” in this region by Hilton and Mang [35], reproduced by Xu *et al.* [36]. The effect arises from the high-spin favoring of highly aligned collective oblate states. Figure 6 reveals that there may be some

evidence for this minimum at  $(\epsilon_2, \gamma) \approx (0.21, -56^\circ)$ . However, at present, we have no clear evidence to support such an interpretation.

## V. SUMMARY

Evidence is presented for two new highly deformed or superdeformed bands in  $^{175}\text{Hf}$ . These sequences are similar to those observed in the neighboring isotopes  $^{168}\text{Hf}$ ,  $^{170}\text{Hf}$ , and  $^{174}\text{Hf}$ . However, because the newly established bands in  $^{175}\text{Hf}$  have been linked into the known level scheme, definite spin assignments have been made for the first time in this region. In this work, these highly deformed bands have been grouped into two classes based on their deformation. The lower deformation band 1 is similar to the triaxial superdeformed bands observed in the Lu nuclei, while band 2 has a higher deformation and is more like the candidate triaxial superdeformed bands observed in the neighboring hafnium isotopes. However, in the present work, no information was

gained in  $^{175}\text{Hf}$  which could be used to reinforce the ideas that the known candidate triaxial superdeformed bands in the Hf region are indeed triaxial.

## ACKNOWLEDGMENTS

Special thanks to D. C. Radford for the use of the RADWARE software [27] and W. T. Milner for the use of the UPAK software [37]. The authors also wish to thank the operations staff at Gammasphere. D.M.C. acknowledges receipt of EPSRC Award No. AF/100225 and D.T.S. acknowledges receipt support from EPSRC. This work was funded by the U.S. Department of Energy Office of Nuclear Physics through Contract Nos. DE-FG02-96ER40983 (University of Tennessee) and W-31-109-ENG-38 (Argonne National Laboratory), USNA Contract No. PHY-0300673, as well as the National Science Foundation, the State of Florida (Florida State University), and the Danish Science Research Council. Useful discussions with J. Simpson are gratefully acknowledged.

- 
- [1] B. Singh, R. Zywna, and R. B. Firestone, Nucl. Data Sheets **97**, 241 (2002).
  - [2] W. Nazarewicz, R. Wyss, and A. Johnson, Nucl. Phys. **A503**, 285 (1989).
  - [3] H. Schnack-Petersen *et al.*, Nucl. Phys. **A594**, 175 (1995).
  - [4] I. Hamamoto and H. Sagawa, Phys. Lett. B **201**, 415 (1988).
  - [5] R. Bengtsson, H. Frisk, F. R. May, and J. A. Pinston, Nucl. Phys. **A415**, 189 (1984).
  - [6] K. Starosta *et al.*, Phys. Rev. Lett. **86**, 971 (2001).
  - [7] S. Frauendorf *et al.*, Nucl. Phys. **A617**, 131 (1997).
  - [8] A. Bohr and B. R. Mottelson, *Nuclear Structure* (World Scientific, Singapore, 1975), Vol. 2.
  - [9] J. Dudek and W. Nazarewicz, Phys. Rev. C **31**, 298 (1985).
  - [10] S. W. Ødegård *et al.*, Phys. Rev. Lett. **86**, 5866 (2001).
  - [11] T. Bengtsson and I. Ragnarsson, Nucl. Phys. **A436**, 14 (1985).
  - [12] T. Bengtsson, Nucl. Phys. **A512**, 124 (1990).
  - [13] R. Bengtsson, T. Bengtsson, M. Bergström, R. Hyde, and G. Hagemann, Nucl. Phys. **A569**, 469 (1994).
  - [14] P. Bringel *et al.*, Eur. Phys. J. A **16**, 155 (2003).
  - [15] W. Schmitz *et al.*, Phys. Lett. B **303**, 230 (1993).
  - [16] D. R. Jensen *et al.*, Nucl. Phys. **A703**, 3 (2002).
  - [17] J. Domscheit *et al.*, Nucl. Phys. **A660**, 381 (1999).
  - [18] S. Törmänen *et al.*, Phys. Lett. B **454**, 8 (1999).
  - [19] G. Schönwaßer *et al.*, Eur. Phys. J. A **15**, 435 (2002).
  - [20] G. Schönwaßer *et al.*, Phys. Lett. B **552**, 9 (2003).
  - [21] H. Amro *et al.*, Phys. Lett. B **553**, 197 (2003).
  - [22] C. X. Jang *et al.*, Eur. Phys. J. A **1**, 237 (1998).
  - [23] H. Amro, Phys. Lett. B **509**, 39 (2001).
  - [24] A. Neußer *et al.*, Eur. Phys. J. A **15**, 439 (2002).
  - [25] M. K. Djongolov *et al.*, Phys. Lett. B **560**, 24 (2003).
  - [26] I. Y. Lee, Nucl. Phys. **A520**, 641c (1990).
  - [27] D. C. Radford, Nucl. Instrum. Methods Phys. Res. A **361**, 297 (1995).
  - [28] F. Kondev *et al.* (unpublished).
  - [29] N. L. Gjørup, Ph.D. thesis, University of Copenhagen, Niels Bohr Institute, Copenhagen, Denmark, 1994.
  - [30] G. D. Dracoulis and P. M. Walker, Nucl. Phys. **A342**, 335 (1980).
  - [31] N. L. Gjørup *et al.*, Z. Phys. A **337**, 353 (1990).
  - [32] K. S. Krane, R. M. Steffen, and R. M. Wheeler, Nucl. Data Tables **11**, 351 (1973).
  - [33] P. Walker and G. Dracoulis, Nature (London) **399**, 35 (1999).
  - [34] D. J. Hartley *et al.* (private communication) 2004.
  - [35] R. R. Hilton and H. J. Mang, Phys. Rev. Lett. **43**, 1979 (1979).
  - [36] F. Xu, P. M. Walker, and R. Wyss, Phys. Rev. C **62**, 014301 (2000).
  - [37] W. T. Milner, computer code UPAK (Oak Ridge Data Analysis Package, ORNL, TN).